

# Construction of Bar-beam Element Based on Daubechies Wavelet and Second-generation Wavelet

Yanxin Liu<sup>a,b</sup>, Wenjian Lan<sup>a</sup>, Xin Zhang<sup>a</sup>, Hanxiang Wang<sup>a\*</sup>

<sup>a</sup> School of Mechanical Engineering, China University of Petroleum, Qingdao 266580, PR China;

<sup>b</sup> School of Petroleum Engineering, China University of Petroleum, Qingdao 266580, PR China.  
[wanghx1996@163.com](mailto:wanghx1996@163.com)

The second-generation wavelet scale function shows the weakness of no expressions, the curve-fitting method is proposed. Bar-beam elements are constructed based on Daubechies wavelet and second-generation wavelet, wavelet function is used to construct interpolation function. The wavelet interpolation coefficient is transformed to physical space through the transformation matrix. Precision validation of the bar-beam elements constructed is conducted by numerical examples. The results show that the wavelet finite element has high precision in solving deformation and strain.

## 1. Introduction

Wavelet finite element method is a new numerical analysis method developed in recent years. It makes up for the shortage that the traditional finite element method (FEM). Also, it has the advantages in solving the singularity which the traditional finite element method is difficult to deal with.

Many scholars have made a lot of researches on wavelet finite element method, but most of the models are plane beam element and plate element. Ko J. (Ko et al, 1995) has formed the wavelet elements, and did some research about one and two dimensional Neumann problems. Chen W. and Wu C. (Chen and Wu, 1995; Chen and Wu, 1996) has solved the truss and membrane vibration problems with wavelet finite element. Ma J. (Ma et al, 2003) constructed a new wavelet-based beam element for the first time, by using the Daubechies wavelet with 12 coefficients scaling function. Chen X. (Chen et al, 2006) found out a method to calculate multiscale connection coefficient. Diaz A. L. (Diaz et al, 2009) found out the feasibility of a hybrid scheme. Multiresolution approach adopting hierarchical bases has been proposed by Yserentant H. (Yserentant, 1986). The second generation method of wavelet collocation for the solution of PDEs was presented by Amaratunga K. and Vasilyev O. V. (Amaratunga and Sudarshan, 2006; Vasilyev and Kevlahan 2005). The current structure of the wavelet plane rigid frame element and wavelet space beam element need to adopt the method of condensation freedom, but this method cannot be used for dynamic calculation. Xiang J. (Xiang et al, 2008) applied the common torsion element shape function to the torsion angle in establishing the dynamic BSWI beam element. Although this method has made success, the calculation accuracy is reduced. In this paper, the plane rigid frame element and space rigid frame element are constructed with Daubechies wavelet and the second generation wavelet. With this method the torsion angle is not needed to be dealt with, the condensation freedom is not needed in statics analysis and the method can be used for dynamic calculation.

## 2. Daubechies wavelet and Second generation wavelet

### 2.1 Daubechies wavelet

Daubechies wavelet was put forward by Belgium female mathematician Daubechies, the N order scale function can be expressed as DN wavelet. There is no clear explicit expression for Daubechies wavelet, the scaling function  $\varphi_N(x)$ , and basis wavelet function  $\psi_N(x)$  are given by the following equation:

$$\varphi_N(x) = \sum_{k=0}^{2N-1} a_N(k) \varphi_N(2x-k) \quad (1)$$

$$\psi_N(x) = \sum_{k=2-2N}^1 b_N(k) \phi_N(2x-k) \quad (2)$$

Where,  $a_N(k)$  is filter coefficient,  $b_N(k) = (-1)^k a_N(1-k)$

## 2.2 Second generation wavelet

The second generation wavelet (SGW) is usually expressed as SGWN ( $N$  is the number of prediction coefficient). The second generation wavelet transform has many advantages such as simple algorithm, high speed of signal decomposition operation, less memory, possibility of perfect reconstruction and analysis of arbitrary length signals. The decomposition algorithm of the SGW transform based on interpolating subdivision is decomposition and reconstruction (Wang et al, 2012).

SGW6 wavelet is adopted to construct one-dimensional element. The SGW wavelet shows no expressions, it would bring a lot of problems when it is used in the finite element calculation. In order to solve the problems, the following fitting function is adopted to calculate the expression of SGW6 and Fig. 1 shows the effect of fitting function.

$$y = 0.0165 + \left[ 1.81038e^{-2.28338(x+8.19225 \times 10^{-9})^2} - \frac{0.96660}{4(x+8.19225 \times 10^{-9})^2 + 1.06608^2} \right] \quad (3)$$

## 3. One-dimension element conversion matrix

In order to satisfy the compatibility and continuity of displacement on the boundary of adjacent element, the element stiffness matrix and mass matrix must be converted to the physical space by wavelet space, and then the corresponding element freedom must be converted to position function from the wave coefficient transformation matrix. Thus, the transformation matrix is introduced which plays an important role in the structure of Daubechies wavelet and the second generation wavelet elements.

Consider one-dimension boundary value:

$$\begin{cases} L(u(x)) = f(x), \Omega = \{x \mid x \in [c, d]\} \\ \text{Boundary condition} \end{cases} \quad (4)$$

In Eq. (4),  $L(\cdot)$  is a differential operator,  $\Omega$  is solving domain,  $\Omega$  is subdivided into many subdomains through the mesh of generation  $\Omega_i$  ( $i=1, 2, \dots$ ), for every subdomain  $\Omega_i$ , it can be mapped as standard solution domain  $\Omega_e = \{\xi \mid \xi \in [0, 1]\}$ .

For axial force rod element and torsion bar element,  $\Omega_i$  (supposing  $\Omega_i = \{x \mid x \in [a, b]\}$ ,  $l_e = b-a$ ) is divided into  $n=2^j+m-2$  ( $j > j_0$ ) parts with the application of Daubechies wavelet scale function as the interpolation function to construct elements. The distribution of element nodes is shown in Figure 1.

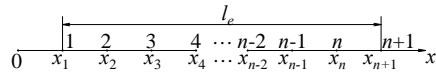


Figure 1: Scatter of subdomain  $\Omega_i$

The node coordinates are  $x_h \in [x_i, x_{n+1}]$ , ( $1 \leq h \leq n=1$ ,  $h \in \mathbb{N}$ )

The conversion equation is defined as:

$$\xi = (x - x_i) / l_e, (0 \leq \xi \leq 1) \quad (5)$$

Then each node  $x_h$  mapping value  $\xi_h$  contents:

$$\xi_h = (x_h - x_i) / l_e, (0 \leq \xi_h \leq 1) \quad (6)$$

Field function  $u(x)$  can be expressed as

$$u(x) = \sum_{i=2-2N}^0 a_i \phi_N(\xi - i) = \Phi \alpha^e \quad (7)$$

In Eq. (7),  $\alpha^e = [\alpha_{2-2N}, \alpha_{3-2N}, \dots, \alpha_0]^T$  is the column vector of the wavelet coefficient.  $\Phi = [\phi_N(\zeta+2N-2), \phi_N(\zeta+2N-3), \dots, \phi_N(\zeta)]$  is scale function vector.

Physical freedom column vector is defined as:

$$\mathbf{u}^e = [u(x_1), u(x_2), \dots, u(x_{n+1})]^T \quad (8)$$

Substitute different factors  $\xi_h$  in Eq. (8) into Eq. (7) respectively

$$\mathbf{u}^e = \mathbf{T}^e \mathbf{a}^e \quad (9)$$

Element conversion matrix in the Equation  $\mathbf{T}^e = [\Phi(\zeta_1), \Phi(\zeta_2), \dots, \Phi(\zeta(n+1))]^T$   
By Eq. (9):

$$\mathbf{a}^e = (\mathbf{T}^e)^{-1} \mathbf{u}^e \quad (10)$$

Substitute to Eq. (7):

$$u(x) = \Phi(\mathbf{T}^e)^{-1} \mathbf{u}^e = \mathbf{N}^e \mathbf{u}^e \quad (11)$$

And

$$\mathbf{N}^e = \Phi \mathbf{R} \quad (12)$$

In Eq. (12),  $\mathbf{N}^e$  is equivalent to the shape function of traditional finite element,  $\mathbf{R} = (\mathbf{T}^e)^{-1}$

The Euler–Bernoulli beam element is constructed with the SGW scale function. In interpolation of deflection  $w$  and angle  $\theta$ , the angle  $\theta$  is not the independent interpolation. However, it is exported by  $dw/dx$ . In order to construct the space beam element which is suitable for the dynamic analysis, each node should include transverse displacement and rotation degrees of freedom. If SGWN wavelet scale function is used, the element is divided into  $r=N-2$  segments, and there are  $r+1$  nodes in each element, the element total degrees of freedom are  $2r+2$ . The element node arrangement is shown in Figure 2.

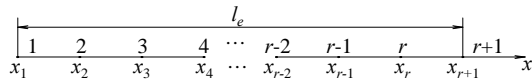


Figure3: Scatter of subdomain  $\Omega_i$

Physical freedom of the element is:

$$\mathbf{w}^e = \left( w(x_1), \frac{dw(x_1)}{dx}, w(x_2), \frac{dw(x_2)}{dx}, \dots, w(x_r), \frac{dw(x_r)}{dx}, w(x_{r+1}), \frac{dw(x_{r+1})}{dx} \right)^T \quad (13)$$

Where,  $dw(x_i)/dx$  is the angle freedom of the element node.

Field functions can be expressed as

$$w(x) = \sum_{i=1}^{2N-2} a_i \phi(\xi + N - 1 - i) = \Phi \mathbf{a}^e \quad (14)$$

In Eq. (14),  $\Phi = [\phi(\zeta+N-2), \phi(\zeta+N-3), \dots, \phi(\zeta-N-1)]$  is scale function vector,  $\mathbf{a}^e = [\alpha_1, \alpha_2, \dots, \alpha_{2N-2}]$  is wavelet coefficient column vector.

Transform matrix can be acquired with the same method:

$$\mathbf{T}_b^e = \left[ \Phi(\xi_1), \frac{1}{l_e} \frac{d\Phi(\xi_1)}{d\xi}, \Phi(\xi_2), \frac{1}{l_e} \frac{d\Phi(\xi_2)}{d\xi}, \dots, \Phi(\xi_r), \frac{1}{l_e} \frac{d\Phi(\xi_r)}{d\xi}, \Phi(\xi_{r+1}), \frac{1}{l_e} \frac{d\Phi(\xi_{r+1})}{d\xi} \right]^T \quad (15)$$

As the same, the shape function can be obtained

$$\mathbf{N}_b^e = \Phi \mathbf{R}_b \quad (16)$$

In Eq. (16),  $\mathbf{R}_b = (\mathbf{T}_b^e)^{-1}$

## 4. Construction of wavelet element

### 4.1 Daubechies wavelet axial force rod element and torsion bar element

D3 wavelet is used to construct Daubechies wavelet axial force rod element and torsion bar element. As for D3 wavelet axial force rod element, there are 5 nodes and 1 degree of freedom in each node:  $u_i$ . As for D3

wavelet torsion bar element, there are 5 nodes and 1 degree of freedom in each node:  $\theta_i$ . Each of them has 5 degrees of freedom.

As shown in Figure 4, it is a constant cross-section rod which is under uniformly distributed load along the axis  $f(x) = 1$ ,  $EA = 1$ ,  $L = 1$ .

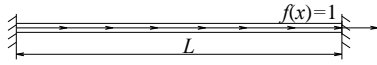


Figure 3: Straight bar

A D3 wavelet rod element is used, and the calculated results are used to predict the deformation and strain values of other locations that are used to compare with the theoretical solution. The results are shown in table 1,  $(L/10)$  represents that the calculated value is used to predict the result in the point of  $x = L/10$ . The maximum error of the calculation of displacement and strain are  $8.5 \times 10^{-5}\%$  and  $5.6 \times 10^{-4}\%$  in the calculating points respectively. And in the prediction location, the maximum error of the calculation of displacement and strain are  $2.3 \times 10^{-4}\%$  and  $1.4 \times 10^{-3}\%$ . From the results, the constructed axial force rod element has high calculation precision. D3 wavelet torsion bar element has the similar calculation precision as D3 wavelet rod element.

Table 1: Results and Errors of D3 wavelet rod element

x	Displacement			Strain		
	Theoretical value	Calculated value	Relative error (%)	Theoretical value	Calculated value	Relative error (%)
0	0	0	—	0.5	0.5000035	$7 \times 10^{-4}$
$(L/10)$	0.045	0.0450001	$2.2 \times 10^{-4}$	0.4	0.3999989	$2.8 \times 10^{-4}$
$(L/6)$	0.06944444	0.06944454	$1.4 \times 10^{-4}$	0.3333333	0.3333332	$3 \times 10^{-5}$
$L/4$	0.09375	0.09374992	$8.5 \times 10^{-5}$	0.25	0.2499986	$5.6 \times 10^{-4}$
$(L/3)$	0.1111111	0.1111110	$9 \times 10^{-5}$	0.1666667	0.1666690	$1.4 \times 10^{-3}$
$L/2$	0.125	0.1249999	$8 \times 10^{-5}$	0	-0.0000007	—
$(2L/3)$	0.1111111	0.1111111	0	-0.1666667	-0.1666661	$3.6 \times 10^{-4}$
$3L/4$	0.09375	0.09375007	$7.5 \times 10^{-5}$	-0.25	-0.2499997	$1.2 \times 10^{-4}$
$(5L/6)$	0.06944444	0.06944460	$2.3 \times 10^{-4}$	-0.3333333	-0.3333323	$2.1 \times 10^{-4}$
L	0	0	—	-0.5	-0.5000005	$1 \times 10^{-4}$

4.2 SGW Euler–Bernoulli beam element

SGW6 wavelet is used to construct SGW Euler–Bernoulli beam element. There are 5 nodes and 2 degrees of freedom in each node:  $w_i$ ,  $\theta_i$ . Each element has 10 degrees of freedom. Figure 4 shows SGW6 Euler–Bernoulli beam element.

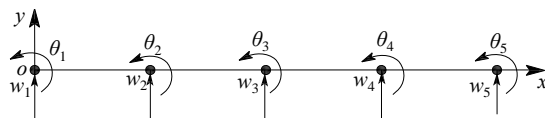


Figure 4: SGW6 Euler–Bernoulli beam element

As shown in Figure 5, it is a uniform cross-section beam, the length is  $L = 1$ , the bending stiffness is  $EI = 1$ , simply supported on both ends. The distributed load is  $q(x) = 1$ .

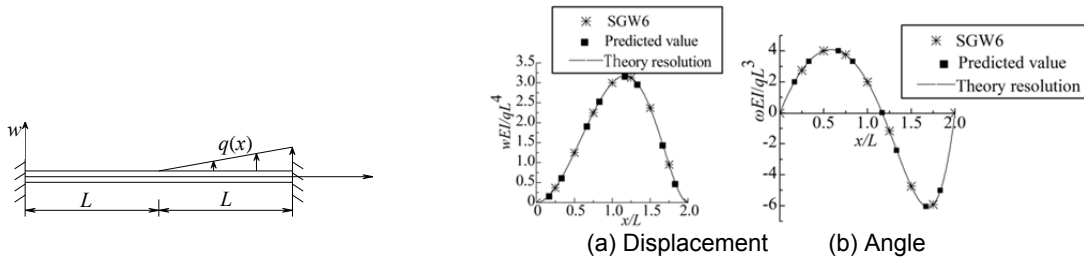


Figure 5: Constant-section local beam

Figure 6: Results of constant section local beam

Two SGW6 Euler beam elements are used, and the results are used to predict the torsion angle values of other locations. As shown in Figure 6, the calculated values and the theoretical values in the calculating points and prediction points respectively are very close.

**4.3 D3-SGW6 space rigid frame element**

There are a D3 axial force rod element, a D3 torsion bar element and two SGW6 Euler–Bernoulli beam elements in a D3-SGW6 space rigid frame element. The element node number is 5. There are 6 degrees of freedom in each node:  $u_i, v_i, w_i, \theta_{ix}, \theta_{iy}, \theta_{iz}$  and each element has 30 degrees of freedom. Figure 7 shows D3-SGW6 space rigid frame element.

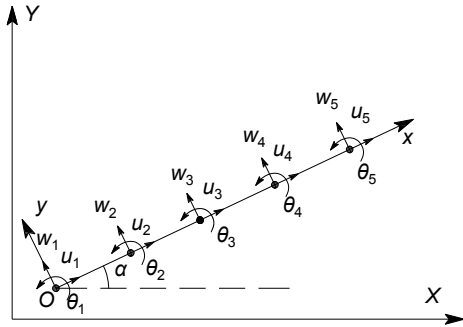


Figure 7: D3-SGW6 plane rigid frame element

As shown in Figure 8, it is plane rigid frame and the frame consists of 5 bars. For each bar, the cross-sectional area is  $A=100\text{cm}^2$ , the inertia moment is  $I=20000\text{cm}^4$  and elastic modulus is  $E=2.1 \times 10^{11}\text{Pa}$ .

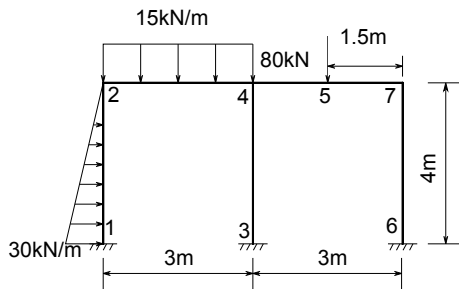


Figure 8: Plane frame with distributed force and concentrated force

Five D3-SGW6 plane frame elements are used to compare with 200 ordinary plane frame elements. The calculated results are shown in Table 2. The results show that the D3-SGW6 plane frame element has high precision and the analysis of D3-SGW6 plane frame element has better efficiency.

Table 2: Displacement analysis of plane frame

Node Number	Displacement in x direction(mm)		Displacement in y direction(mm)		Angle (°)	
	traditional element	Wavelet element	traditional element	Wavelet element	traditional element	Wavelet element
2	0.78838727	0.78838730	-0.03109088	-0.03109088	-0.03446829	-0.03446825
4	0.77076680	0.77076684	-0.12998035	-0.12998034	-0.25207545	-0.25207546
7	0.75614577	0.75614580	-0.07702401	-0.0770240	0.27175096	0.27175095
Maximum error (%)	$5.2 \times 10^{-8}$		$7.7 \times 10^{-6}$		$1.2 \times 10^{-4}$	

**5. Conclusion**

The SGW scale function shows the faults of no expression, therefore the fitting function method is proposed. The use of the fitting method could be reasonable from the calculation precision of the correlation coefficients and the tectonic elements.

The axial force element and torsion bar element are constructed with Daubechies wavelet. The Euler–Bernoulli beam element is constructed with the second generation wavelet. The plane rigid frame element and space rigid frame element are constructed with the hybrid wavelet of the above two kinds of wavelet. The calculation accuracy is verified by numerical examples. The results show that the wavelet element has high calculation accuracy.

### Acknowledgement

This work was financially supported by Natural fund of Shandong Province (Approval No. ZR2015EL012), Qing Dao City Applying Fundamental Research Project (Approval No. 14-2-4-64-jch).

### References

- Amaratunga K., Sudarshan R., 2006, Multiresolution modeling with operator-customized wavelets derived from finite elements, *Computer Methods in Applied Mechanics and Engineering*, 195, 2509-2531, DOI: 10.1016/j.cma.2005.05.012.
- Chen W., Wu C., 1995, A spline wavelets element method for frame structures vibration, *Computational Mechanics*, 16, 11-21, DOI: 10.1007/BF00369881.
- Chen W., Wu C., 1996, Adaptable spline element for membrane vibration analysis, *International Journal for Numerical Methods in Engineering*, 39, 2457-2476, DOI: 10.1002/(SICI)1097-0207(19960730)39:14<2457::AID-NME961>3.0.CO;2-J.
- Chen X., He Z., Xiang J., Li B., 2006, A dynamic multiscale lifting computation method using Daubechies wavelet, *Journal of Computational and Applied Mathematics*, 188, 228-245, DOI: 10.1016/j.cam.2005.04.015.
- Diaz A.L., Martin M.T., Vampa V., 2009, Daubechies wavelet beam and plate finite elements, *Finite Elements in Analysis and Design*, 45, 200-209, DOI: 10.1016/j.finel.2008.09.006.
- Ko J., Kurdila A. J., Pilant M. S., 1995, A class of finite element methods based on orthonormal, compactly supported wavelets, *Computational Mechanics*, 16, 235-244, DOI: 10.1007/BF00369868.
- Ma J., Xue J., Yang S., He Z., 2003, A study of the construction and application of a Daubechies wavelet-based beam element, *Finite Elements in Analysis and Design*, 39, 965-975, DOI: 10.1016/S0168-874X(02)00141-5.
- Vasilyev O.V., Kevlahan K.R., 2005, An adaptive multilevel wavelet collocation method for elliptic problems, *Journal of Computational Physics*, 206, 412- 431, DOI: 10.1016/j.jcp.2004.12.013
- Wang Y., Chen X., He Z., 2012, A second-generation wavelet-based finite element method for the solution of partial differential equations, *Applied Mathematics Letters*, 25, 1608-1613, DOI: 10.1016/j.aml.2012.01.021.
- Xiang J., Yang L., Zhang Y., Chen X., He Z., 2008, Dynamic analysis of flexible rotor based on wavelet finite element method, *Journal of vibration and shock*, 27, 1-5, DOI: 10.13465/j.cnki.jvs.2008.09.015.
- Yserentant H., 1986, On the multi-level splitting of finite element spaces, *Numerische Mathematik*, 49, 379-412, DOI: 10.1007/BF01389538.